Z-lineshape versus 4th generation masses.

S. S. Bulanov [*], V. A. Novikov [†], L. B. Okun [‡],
ITEP, Moscow, Russia
A. N. Rozanov [§],
CPPM, IN2P3, CNRS, Univ. Mediteranee, Marseilles, France
and ITEP, Moscow, Russia
M. I. Vysotsky [¶],
ITEP, Moscow, Russia.

Abstract

The dependence of the Z-resonance shape on the location of the threshold of the $N\bar{N}$ production (N is the 4th generation neutrino) is analyzed. The bounds on the existence of 4th generation are derived from the comparison of the theoretical expression for the Z-lineshape with the experimental data. The 4th generation is excluded at 95% C. L. for $m_N < 46.7 \pm 0.2$ GeV.

1 Introduction

The straightforward generalization of the Standard Model through the inclusion of extra chiral generations of heavy leptons (N, E) and quarks (U, D) was studied in a number of papers [1]. The bounds on the existence of the 4th generation from the analysis of the electroweak data fit were obtained in [1–5]. However, the dependence of Z-resonance shape on the contribution of 4th generation and, in particular, on the location of the threshold

[*]bulanov@heron.itep.ru
[†]novikov@heron.itep.ru
[‡]okun@heron.itep.ru
[§]rozanov@cppm.in2p3.fr
[¶]vysotsky@heron.itep.ru

of $N\bar{N}$ production was not considered in [2–5], because the results were obtained in the Breit-Wigner approximation. This approximation is valid for the thresholds of 4th generation particles production being far from m_Z. If the threshold location approaches m_Z ($m_N \to m_Z/2$), than one gets a fast worsening of the fit (see Fig. 4 of [4]). It is due to the fact that the standard approach to the radiative corrections to the electroweak observables, used in [1–5], does not work in the presence of the heavy neutrino (N) with $m_N - m_Z/2 < \Gamma_Z$. After Taylor expansion over $p^2 - m_Z^2$ the expression for the polarization operator tends to infinity for $m_N \to m_Z/2$, because the point, at which the Taylor expansion is performed, becomes the branch point of the polarization operator.

According to the results of [2–5] the best fit corresponds to $m_N \approx 50$ GeV, that is why careful analysis of the region $m_N \approx m_Z/2$ is undertaken in this paper. We study the dependence of the Z-lineshape on the location of the threshold of $N\bar{N}$ production. We analyze the energy dependence of $e^+e^- \to Z \to hadrons$ cross section near Z-resonance and find that it exhibits a characteristic behavior near the threshold, a casp [1]. The casp is caused by the square root ($\sqrt{s - 4m_N^2}$), appearing in the contribution of 4th generation neutrino to the polarization operator of Z-boson. The form of the casp is determined by the location of the threshold with respect to m_Z.

Then we compare the theoretical expression for the Z-lineshape with the experimental data , presented in [11], using the ZFITTER [12] in order to take into account the electromagnetic corrections, and find that the 4th generation is excluded at 95% C. L. for $m_N < 46.7 \pm 0.2$ GeV. This bound depends on the masses of the charged 4th generation particles and on the mass of the higgs. Using the results of [5], we fix the mass of the charged lepton (E) and take into account that the splitting of quark masses and higgs mass are not independent. This leaves us with one free parameter – the splitting of quark masses, which we vary from 0 to 50 GeV. This variation is the source of the theoretical uncertainty in the bound on N mass as well as the uncertainties of the input parameters of ZFITTER. Note, that the $\chi^2/n_{d.o.f.}$ for the Z-lineshape with 4th generation is even better for certain region of mass values

[1]Such behaviour of the cross section in quantum mechanics was discovered by Wigner, Baz and Breit and is discussed in textbook [9]. In particle physics analogous phenomenon was considered in [10]. Unlike cases analyzed previously, Z-boson physics is purely perturbative, allowing to get explicit formulae for cross section. However, being perturbative the variation of cross section because of the casp are small. Nevertheless, high precision of experimental data on Z production allow us to bound N mass from below.

then the $\chi^2/n_{d.o.f.}$ for the SM prediction.

The paper is organized as follows. In section 2 we discuss the general behaviour of the cross-sections near threshold. In section 3 the exact formulae for the contributions of 4th generation particles to the cross section of $e^+e^- \to$ *hadrons* are presented. We study the behavior of the $e^+e^- \to$ *hadrons* cross section near the threshold of $N\bar{N}$ production in section 4. Using the result of section 3 we compare our prediction for the Z-lineshape in the presence of 4th generation with the experimental data in section 5. The conclusions are presented in section 6.

2 The cross-sections near threshold.

Let's consider the interaction of two particles A and B, which form some resonance R, which in its turn decays into a system of particles f (see Fig. 1). The behavior of the cross section of this process near R-peak can be calculated in the general case, regardless of the exact form of interaction. We need only the partial width of particle R. The cross section near the resonance is described by the Breit-Wigner formula [12]:

$$\sigma = \frac{4\pi s^2}{I^2} \frac{2S_R+1}{(2S_A+1)(2S_B+1)} \frac{\Gamma_{R\to A+B}\Gamma_{R\to f}}{(s-M^2)^2+\Gamma^2 s^2/M^2} \frac{s}{M^2}, \tag{1}$$

where $s=(p_A+p_B)^2$, M and Γ are mass and total width of R correspondingly, $I = 1/2\sqrt{(s-(m_A+m_B)^2)(s-(m_A-m_B)^2)}$. S_R, S_A and S_B are spins of particles R, A and B correspondingly.

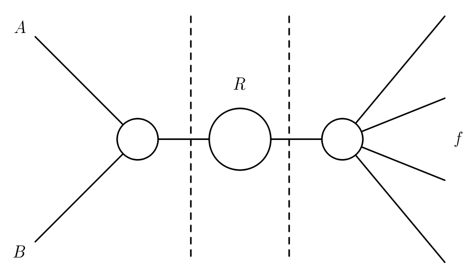

Figure 1: The reaction $A+B \to R \to f$.

Let's consider the case when the reaction occurs not only near resonance, but also near the threshold of $N\bar{N}$ production. In order to study this effect we write explicitly the contribution of the $N\bar{N}$ loop to the propagator of particle R:

$$\frac{1}{s - M^2 + i\Gamma s/M + \Sigma_R^{(N)}(s)}, \tag{2}$$

the imaginary part of polarization operator $\Sigma_R^{(N)}(s)$ is connected with the $R \to N\bar{N}$ decay probability by the unitarity relation. The decay probability is proportional to $\sqrt{s - 4m_N^2}$, the factor that arises from the integration over phase space. Then, if we rewrite the polarization operator as $\Sigma_R^{(N)}(s) = a + ib\sqrt{s - 4m_N^2}$, and expand the expression for the propagator near $s = 4m_N^2$, it will take the following form

$$T_0 + iT_1\sqrt{s - 4m_N^2}, \tag{3}$$

where T_0 and T_1 are some functions of a, b, s, m_Z^2, Γ_Z. Then the cross-section is proportional to [9]

$$\begin{aligned} \sigma \sim |T_0|^2 + 2\sqrt{s - 4m_N^2}\,\Im[T_0 T_1^*], &\qquad s > 4m_N^2 \\ |T_0|^2 - 2\sqrt{4m_N^2 - s}\,\Re[T_0 T_1^*], &\qquad s < 4m_N^2. \end{aligned} \tag{4}$$

The form of the cross-section energy behavior near threshold is defined by the value of the angle, $arg(T_0) - arg(T_1)$ (see Fig. 2) [9]. In all cases there are two branches lying on both sides of common vertical tangent. Thus, the existence of the reaction threshold leads to the appearance of the characteristic energy dependence of the cross section. The cross section near threshold is the linear function of $\sqrt{s - 4m_N^2}$ with different slopes under and above threshold. The existence of the square root branch point, $s = 4m_N^2$, prevents the amplitude expansion near branch point in Taylor series.

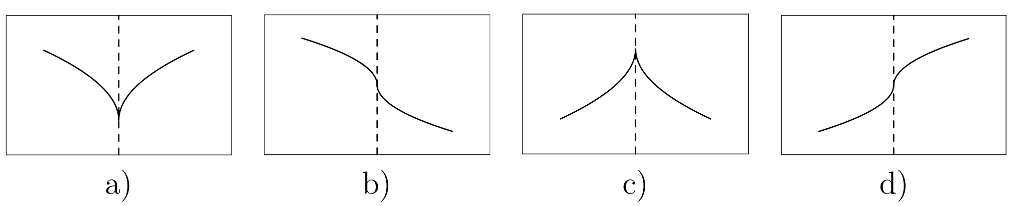

Figure 2: Different cases of cross section behavior near threshold. Vertical axis is σ, while horizontal one is s; dashed line crosses horizontal axis at $4m_N^2$

Below we will consider the case when $R \equiv Z$.

3 Polarization operator.

The cross-section of $e^+e^- \to Z \to hadrons$ near Z-resonance is well described by the Breit-Wigner formula [12]

$$\sigma_h^{SM} = \frac{12\pi\Gamma_e\Gamma_h}{|p^2 - m_Z^2 + i\Gamma_Z^{SM} p^2/m_Z|^2} \frac{p^2}{m_Z^2}, \tag{5}$$

where $p = p_1 + p_2$, p_1 and p_2 are momenta of initial electron and positron, m_Z is the mass of Z boson, Γ_e is the width of $Z \to e^+e^-$ decay, Γ_h is the width of $Z \to hadrons$, Γ_Z^{SM} is the total width of Z in the SM.

The 4th generation contributes to the Z-boson polarization operator. This contribution can be accounted for in the expression (5) by replacing the denominator:

$$|p^2 - m_Z^2 + i\Gamma_Z^{SM} p^2/m_Z|^2 \to$$
$$|p^2 - m_Z^2 + i\Gamma_Z p^2/m_Z + \Sigma_Z^{(4th)}(p^2) - \Re[\Sigma_Z^{(4th)}(m_Z^2)]|^2, \tag{6}$$

where the subtraction is performed due to the fact that we follow the approach of [2–4] and use for m_Z, α and G_F experimental values. Thus the renormalization scheme is on-shell one. The real part of the polarization operator at $s = m_Z^2$ is subtracted in order to avoid the shifting of Z-boson mass. It is due to the fact that the real part of the polarization operator contributes to m_Z.

$$\Sigma_Z^{(4th)}(p^2) = \Sigma_Z^{(N)}(p^2) + \Sigma_Z^{(E)}(p^2) + \Sigma_Z^{(U)}(p^2) + \Sigma_Z^{(D)}(p^2) \tag{7}$$

is the contribution of the 4th generation to Z polarization operator. The contribution of the $N\bar{N}$ channel into Z width is taken into account by the imaginary part of $\Sigma_Z^{(N)}(p^2)$.

Note, that Γ_Z in (6) includes decays of Z into particles of the first three generations. The 4th generation also influences Γ_Z in non-direct way. It is due to the fact that the polarization operators of gauge bosons enter the radiative corrections for g_A and g_V, which in their turn enter the amplitude of the Z-boson decay into fermion-antifermion pair:

$$M(Z \to f\bar{f}) = \frac{1}{2}\bar{f} Z_\alpha \bar{\psi}_f(\gamma_\alpha g_{Vf} + \gamma_\alpha\gamma_5 g_{Af})\psi_f, \tag{8}$$

where $\bar{f}^2 = 4\sqrt{2}G_\mu m_Z^2 = 0.54866(4)$, G_μ is Fermi coupling constant. In the case of the Z decay into $\nu\bar{\nu}$ the contribution of final state interaction equals zero and

$$\Gamma_\nu = 4\Gamma_0(g_{V\nu}^2 + g_{A\nu}^2), \tag{9}$$

where $\Gamma_0 = G_\mu m_Z^3/24\sqrt{2}\pi$ is the so called "standard" width. If we neglect the masses of neutrinos then $g_{V\nu} = g_{A\nu} = g_\nu$. For the decay into any pair of charged leptons we get:

$$\Gamma_l = 4\Gamma_0 \left[g_{Vl}^2 \left(1 + \frac{3\bar{\alpha}}{4\pi}\right) + g_{Al}^2 \left(1 + \frac{3\bar{\alpha}}{4\pi} - 6\frac{m_l^2}{m_Z^2}\right)\right], \tag{10}$$

where m_l is the mass of the lepton, $\bar{\alpha} \equiv \alpha(m_Z^2) = [128.896(90)]^{-1}$. The situation slightly changes in the case of $Z \to q\bar{q}$. There appear the radiative corrections (R_{Vq} and R_{Aq}) due to gluon exchange and emission in the final state:

$$\Gamma_q = 12\Gamma_0 \left(g_{Vq}^2 R_{Vq} + g_{Aq}^2 R_{Aq}\right). \tag{11}$$

According to the results of [8] the one-loop expressions for g_{Al} and $R_l = g_{Vl}/g_{Al}$ are

$$g_{Al} = -\frac{1}{2} - \frac{3\bar{\alpha}}{64\pi s^2 c^2} V_A, \quad R_l = 1 - 4s^2 + \frac{3\bar{\alpha}}{4\pi(c^2 - s^2)} V_R, \tag{12}$$

$$g_\nu = \frac{1}{2} + \frac{3\bar{\alpha}}{64\pi s^2 c^2} V_\nu, \tag{13}$$

and in the case of quarks

$$g_{Aq} = T_{3q}\left[1 + \frac{3\bar{\alpha}}{32\pi s^2 c^2} V_{Aq}\right], \quad R_q = 1 - 4|Q_q|s^2 + \frac{3\bar{\alpha}|Q_q|}{4\pi(c^2 - s^2)} V_{Rq}, \tag{14}$$

where $c \equiv \cos\theta_{eff}$ and $s \equiv \sin\theta_{eff}$.

The exact expressions for V_A, V_R, V_{Aq} and V_{Rq} in SM can be found in [8].

The 4th generation particles contribute to physical observables through polarization operators of gauge bosons, as it was mentioned above. This gives corrections δV_i to the functions V_i $(i = A,\ R)$ [2].

$$\begin{aligned}
\frac{3\bar{\alpha}}{16\pi s^2 c^2}\delta V_A &= \Pi_Z^{(4th)}(m_Z^2) - \Pi_W^{(4th)}(0) - \Sigma_Z^{(4th)\prime}(m_Z^2), \\
\frac{3\bar{\alpha}}{16\pi s^2 c^2}\delta V_R &= \left[\Pi_Z^{(4th)}(m_Z^2) - \Pi_W^{(4th)}(0) - \Sigma_\gamma^{(4th)\prime}(0)\right] \\
&\quad - \frac{sc(c^2 - s^2)}{s^2 c^2}\Pi_{\gamma Z}^{(4th)}(m_Z^2),
\end{aligned} \tag{15}$$

where $\Pi_Z(m_Z^2) = \Sigma_Z(m_Z^2)/m_Z^2$. Note that all singular terms, proportional to $1/\varepsilon$ ($\varepsilon = D-4$), in right hand side of eq. (15), arising from polarization operators, cancel, as it was shown in [8]. Thus, the expressions (15) are finite. However, these formulae work well for the new particles being much heavier than Z-boson. If $m_N \to m_Z/2$ then $\Sigma_Z^{(4th)\prime}(m_Z^2)$ tends to infinity. $\Sigma_Z^{(4th)\prime}(m_Z^2)$ comes from the Taylor expansion of Z-boson polarization operator near m_Z. In order to get rid of this unphysical infinity, which arise due to the fact that the expansion is performed at the branch point of the polarization operator, we use the exact expression for the contribution of 4th generation particles to the Z-boson polarization operator.

For the contribution of the 4th generation particles we get

$$\Pi_Z^{(\phi)}(p^2) = \frac{N_c\bar{\alpha}}{8\pi s^2 c^2}\left[\Delta_\phi + 4g_{A\phi}^2\frac{m_\phi^2}{p^2}F\left(\frac{m_\phi^2}{p^2}\right)\right.$$
$$\left.-\frac{2(g_{A\phi}^2+g_{V\phi}^2)}{3}\left((1+2\frac{m_\phi^2}{p^2})F\left(\frac{m_\phi^2}{p^2}\right)+\frac{1}{3}\right)\right], \tag{16}$$

where $\phi =$N, E, U, D; $N_c = 3$ for quarks and $N_c = 1$ for leptons; $\Sigma_Z^{(\phi)}(p^2) = p^2\Pi_Z^{(\phi)}(p^2)$;

$$F(x) = \left[-2 + 2\sqrt{4x-1}\arctan\frac{1}{\sqrt{4x-1}}\right], \tag{17}$$

Δ_ϕ are singular parts:

$$\Delta_\phi = 2\left(\frac{1}{3}(g_{A\phi}^2+g_{V\phi}^2) - 2g_{A\phi}^2\frac{m_\phi^2}{p^2}\right)\left(\frac{1}{\varepsilon} - \gamma + \ln 4\pi - \ln\frac{m_\phi^2}{\mu^2}\right), \tag{18}$$

where $\varepsilon \to 0$, $\gamma = -\Gamma'(1) = 0.577...$, μ is the parameter with dimension of mass, which is needed to preserve the dimensionality of the initial integral.

Let's consider the contribution of N to g_A and g_V. $\Sigma_Z'(m_Z^2)$ arises in g_A due to the renormalization of Z-boson wave function. In order to avoid infinities we will expand near m_Z only singular part of the polarization operator, i. e.

$$p^2 - m_Z^2 + \Sigma_Z(p^2) =$$
$$= (1+\Sigma_Z'(m_Z^2)\Big|_s)[p^2 - m^2(1-\Pi_Z(m^2)\Big|_s - \frac{p^2}{m^2}\,\Pi_Z(p^2)\Big|_{FP})], \tag{19}$$

where index s denotes singular part and index FP – finite part. Then in equations (15) we should replace $\Sigma'(m_Z^2)_Z$ by $\Sigma'(m_Z^2)_Z|_s$ and $\Pi(m_Z^2)_Z$ by

$\Pi_Z(m^2)_Z|_s + \frac{p^2}{m_Z^2}\,\Pi_Z(p^2)|_{FP}$. The combination of singular terms in the resulting expression is the same as in (15) and that's why they cancel each other.

Let's consider the expression for the $e^+e^- \to hadrons$ cross section in the presence of the 4th generation. The singular part of the polarization operator is absorbed in partial widths Γ_e and Γ_h and also in total width of Z, Γ_Z.

$$\frac{\Gamma_e^0\Gamma_h^0}{|p^2 - m_Z^2 + i\Gamma_Z^0 p^2/m_Z + \Sigma^{(4th)}(p^2) - \Re[\Sigma^{(4th)}(m_Z^2)]|^2}$$
$$= \frac{\Gamma_e^0\Gamma_h^0}{(1+\Sigma'|_s)^2|p^2 - m_Z^2 + \frac{i\Gamma_Z^0 p^2}{(1+\Sigma'|_s)m_Z} + (\Sigma^{(4th)}(p^2) - \Re[\Sigma^{(4th)}(m_Z^2)])_{FP}|^2}$$
$$= \frac{\Gamma_e\Gamma_h}{|p^2 - m_Z^2 + i\Gamma_Z p^2/m_Z + (\Sigma^{(4th)}(p^2) - \Re[\Sigma^{(4th)}(m_Z^2)])_{FP}|^2}, \quad (20)$$

where $\Gamma_e = \Gamma_e^0/(1+\Sigma'|_s)$, $\Gamma_h = \Gamma_h^0/(1+\Sigma'|_s)$, $\Gamma_Z = \Gamma_Z^0/(1+\Sigma'|_s)$ and we used the decomposition

$$\Sigma^{(4th)}(p^2) - \Re[\Sigma^{(4th)}(m_Z^2)]$$
$$= (\Sigma^{(4th)}(p^2) - \Re[\Sigma^{(4th)}(m_Z^2)])_s + (\Sigma^{(4th)}(p^2) - \Re[\Sigma^{(4th)}(m_Z^2)])_{FP}$$
$$= \Sigma'(m_Z^2)\Big|_s (p^2 - m_Z^2) + (\Sigma^{(4th)}(p^2) - \Re[\Sigma^{(4th)}(m_Z^2)])_{FP}$$

The cancellation of the singularities is due to the fact that Γ_e, Γ_h and Γ_Z are proportional to $\bar{f}_0^2$, which can be rewritten in terms of G_μ, m_Z and polarization operators as in [8]:

$$\bar{f}_0^2 = 4\sqrt{2}G_\mu m_Z^2[1 - \Pi_W(0) + \Pi_Z(m_Z^2) - D], \quad (21)$$

where D comes from the radiative corrections to G_μ [8]. If we divide $\bar{f}_0^2$ by $(1+\Sigma^{(s)\prime})$ then the resulting expression will be finite, due to the fact that all singular terms cancel. Thus, in the expression for the cross section of $e^+e^- \to hadrons$ there are no singular terms.

We should note, that there is an ambiguity in the definition of singular and finite parts of the polarization operator. The constant term, proportional to $\bar{\alpha}$, can be added to singular part and subtracted from finite part:

$$\Pi_Z(p^2) = \left(\Pi_Z(p^2)\Big|_s + a\bar{\alpha}\right) + \left(\Pi_Z(p^2)\Big|_{FP} - a\bar{\alpha}\right).$$

However, this ambiguity does not affect the expression for the cross section. It is obvious from the following expressions:

$$\frac{\Gamma_e^0\Gamma_h^0}{(1+\Sigma'|_s+a\bar{\alpha})^2|p^2-m_Z^2+\frac{i\Gamma_Z^0 p^2}{(1+\Sigma'|_s)m_Z}+\hat{\Sigma}-a\bar{\alpha}(p^2-m_Z^2)|^2}$$

$$=\frac{\Gamma_e'\Gamma_h'}{|(p^2-m_Z^2)(1-a\bar{\alpha})+\frac{i\Gamma_Z' p^2}{m_Z}+\hat{\Sigma}|^2}=\frac{\Gamma_e'\Gamma_h'/(1-a\bar{\alpha})^2}{|(p^2-m_Z^2)+\frac{i\Gamma_Z' p^2}{(1-a\bar{\alpha})m_Z}+\hat{\Sigma}|^2}$$

$$=\frac{\Gamma_e\Gamma_h}{|(p^2-m_Z^2)+\frac{i\Gamma_Z p^2}{m_Z}+\hat{\Sigma}|^2},$$

where $\hat{\Sigma}=(\Sigma^{(4th)}(p^2)-\Re[\Sigma^{(4th)}(m_Z^2)])_{FP}$,

$$\Gamma_i=\frac{\Gamma_i'}{1-a\bar{\alpha}}=\frac{\Gamma_i^0}{(1+\Sigma'|_s+a\bar{\alpha})(1-a\bar{\alpha})}=\frac{\Gamma_i^0}{1+\Sigma'|_s+a\bar{\alpha}-a\bar{\alpha}}$$

$$=\frac{\Gamma_i^0}{(1+\Sigma'|_s)},$$

where $i=e,h,Z$.

4 Z-lineshape in the presence of 4th generation.

According to the results of the previous section, the amplitude of $e^+e^-\to$ *hadrons* is proportional to

$$A_h\sim\left[p^2-m_Z^2+i\Gamma_Z^0 p^2/m_Z+\Sigma_Z^{(4th)}(p^2)-\Re(\Sigma_Z^{(4th)}(m_Z^2))\right]^{-1}. \tag{22}$$

In order to study the behavior of the cross section near the threshold qualitively, we shall neglect the contributions of U, D and E to $\Sigma_Z^{(4th)}(p^2)$ as well as the contribution of all 4th generation particles to g_A and g_V. Then the expression (22) takes the following form:

$$A_h\sim\left[p^2-m_Z^2+i\Gamma_Z p^2/m_Z+(\Sigma_Z^{(N)}(p^2)-\Re[\Sigma_Z^{(N)}(m_Z^2)])_{FP}\right]^{-1}. \tag{23}$$

Expanding this expression near the threshold of $N\bar{N}$ production ($p^2 = 4m_N^2$, $A_h \sim T_0 + iT_1\sqrt{p^2 - 4m_N^2}$) we obtain for the cross section the following behaviour

$$\sigma_{p^2<4m_N^2} \sim \frac{1}{\gamma}\left(1 + \frac{\bar{f}^2 m_Z^2}{64\pi}\frac{(4m_N^2 - m_Z^2)\sqrt{\frac{4m_N^2}{p^2} - 1}}{\gamma}\right), \tag{24}$$

$$\sigma_{p^2>4m_N^2} \sim \frac{1}{\gamma}\left(1 - \frac{\bar{f}^2 m_Z^2}{64\pi}\frac{m_Z\Gamma_Z\sqrt{1 - \frac{4m_N^2}{p^2}}}{\gamma}\right), \tag{25}$$

where $\gamma = (4m_N^2 - m_Z^2)^2 + (m_Z\Gamma_Z)^2$ and the second terms in the brackets in eqns. (24, 25) are proportional to $\Re[T_0T_1^*]$ and $\Im[T_0T_1^*]$ respectively. As it was mentioned in section 2 the form of the p^2 dependence of the cross section near the threshold is determined by the relative phase of T_0 and T_1. In our case we have two types of casps (see Figs. 3), which correspond to $argT_0 - argT_1$ lying in the third quadrant for $4m_N^2 < m_Z^2$ and in fourth quadrant for $4m_N^2 > m_Z^2$, or to $\Re[T_0T_1^*]$ and $\Im[T_0T_1^*]$ being negative for $4m_N^2 < m_Z^2$ and $\Re[T_0T_1^*]$ being positive, while $\Im[T_0T_1^*]$ being negative for $4m_N^2 > m_Z^2$. It can also be seen from Figs. 3 that the cross section of $e^+e^- \to hadrons$ decreases above the threshold in accordance with the unitarity.

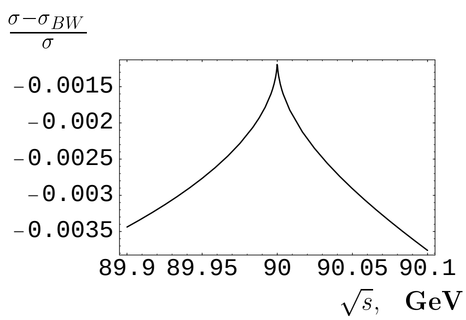

a)

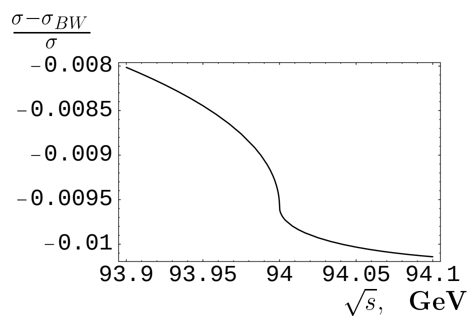

b)

Figure 3: The dependence of relative departure of the $e^+e^- \to hadrons$ cross section in the presence of 4th generation from the SM prediction on the c.m. energy of e^+e^- for $m_N = 45$ GeV (a) and $m_N = 47$ GeV (b).

Though the change of Z-lineshape due to these casps is very small compared to the pure Breit-Wigner curve, as it is shown in Fig. 3, this effect may manifest itself when comparing the theoretical predictions with the experimental data. It is due to the fact, that Z-lineshape is measured with very high precision. In the next section we will compare the theoretical cross section with the experimental data.

5 Comparison with the experiment.

The experimental data on the cross section of $e^+e^- \to hadrons$ reaction is usually presented in the form, that includes the electromagnetic corrections, i. e. initial and final state interactions and photon emission [11]. In order to compare our formulae for the cross section with experimental ones, we use the ZFITTER code [12], which takes into account these corrections. We use the following inputs:

$$m_Z = 91.1882(22)\ \text{GeV}, \quad m_t = 175(4.4)\ \text{GeV}, \quad \bar{\alpha} = 1/128.918(45),$$

$$\alpha_s = 0.1182(27), \quad m_H = 120\ \text{GeV}.$$

With the reasonable assumption that the inital and final state radiation effects are not significantly modified by fourth generation we can calculate the cross section

$$\sigma_h^{th} = \sigma_h \frac{\sigma_h^{ZF}}{\sigma_h^{SM}}, \tag{26}$$

where σ_h^{ZF} is the result of ZFITTER code and

$$\sigma_h = \frac{12\pi\Gamma_e\Gamma_h}{|p^2 - m_Z^2 + i\Gamma_Z p^2/m_Z + (\Sigma^{(4th)}(p^2) - \Re[\Sigma^{(4th)}(m_Z^2)])_{FP}|^2} \frac{p^2}{m_Z^2}, \tag{27}$$

at values of c. m. energy, at which the experimental values of cross section were measured [11]. There are 35 experimental points from 1995 data, which we use. These points are extracted from Fig. 2 of [11] and presented in Table 1. We took only the points corresponding to 1993-1995 set, due to the fact that they are measured with higher precision than the 1991-1993 set. Then we calculate the $\chi^2/n_{d.o.f.}$, where $n_{d.o.f.} = 35 - N$, N is the number of fitted parameters[2], and

$$\chi^2 = \sum_{i=1}^{35} \left(\frac{\sigma_h^{th} - \sigma_h^{exp}}{\delta\sigma_h^{exp}} \right)^2, \tag{28}$$

[2] In our case $N = 1$, because only heavy neutrino mass is a free parameter, all other parameters are fixed.

σ_h^{exp} is the experimental value of cross section and $\delta\sigma_h^{exp}$ is its error, in order to determine at what confidence level the 4th generation is excluded by the experimental data. However, the bound on N mass from below depends on the higgs mass and mass splittings between U and D quarks and between E and N leptons. The effects of varying m_H, $|m_U - m_D|$, and $|m_E - m_N|$ are not independent. As it was shown in [5], the increase of $|m_U - m_D|$ or $|m_E - m_N|$ can be compensated by the increase of higgs mass. This leads to the appearance of χ^2_{min} valleys. It can be seen from Figs. 4a) and 4b), where the dependence of χ^2 on $m_H, |m_U - m_D|$ (a) and $m_H, |m_E - m_N|$ (b) is shown for $m_N = 49$ GeV.

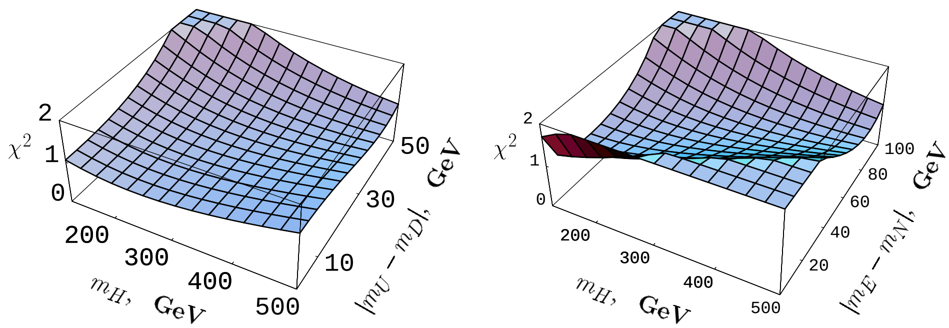

a) b)

Figure 4: The dependence of χ^2 on m_H, $|m_U - m_D|$ (a) and on m_H, $|m_E - m_N|$.

If we use then the LEP II bound $m_E > 100$ GeV and the results of [5], that the best fit of electroweak data corresponds to the light E near the bound and $m_N \approx 50$ GeV, then we have only two parameters, m_H and $|m_U - m_D|$ that affect the bound on m_N. As it can be seen from Fig. 5a) the best fit is acquired for $0.11m_H - 19.7 < |m_U - m_D| < 0.12m_H - 9.2$. In this region of masses we calculate χ^2 and find that the 4th generation is excluded at 95% C. L. for $m_N < 46.7 \pm 0.2$ GeV. The theoretical uncertainty is caused by the varying of $|m_U - m_D|$ from 0 to 50 GeV, as well as by the uncertainties of the input parameters of ZFITTER, which were also used when calculating σ_h and σ_h^{SM}. The main contribution to the theoretical uncertainty comes from m_t and α_S. The variation from 0 to 50 GeV is chosen, because the quality of the fit is fast worsening for $|m_U - m_D| > 50$ GeV.

In order to illustrate the dependence of the fit quality on the higgs mass we study $\chi^2(m_N, m_H)$ (see Fig. 5b)). From this figure it is seen that the 95% C. L. bound lies below 50 GeV and slightly varies with the increase of the

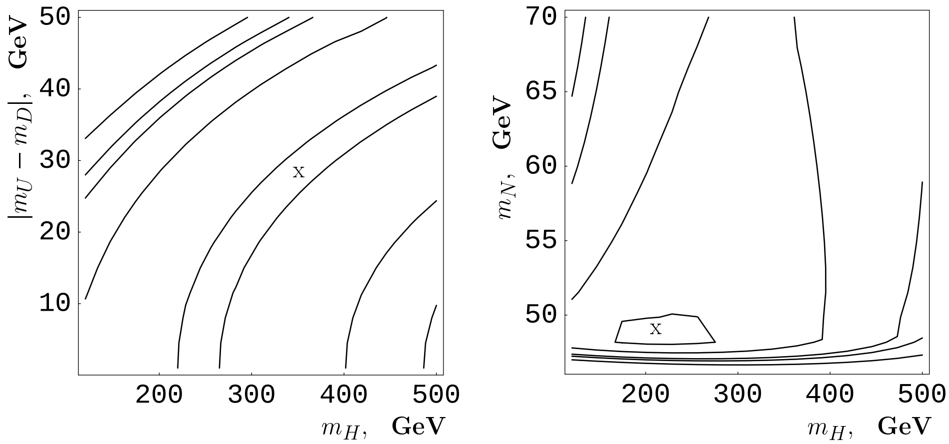

a) b)

Figure 5: a) Exclusion plot on the plane m_H, $|m_U - m_D|$ for $m_N = 49$ GeV; $\chi^2_{min} = 0.85$ denoted by cross b) Exclusion plot on the plane m_H, m_N for $|m_U - m_D| = 10$ GeV; $\chi^2_{min} = 0.85$ denoted by cross. Solid lines represents the borders of 1σ, 2σ, 3σ, 4σ and 5σ regions.

higgs mass near $m_N = 47$ GeV. In this figure we take $|m_U - m_D| = 10$ GeV. It can be seen from Figs. 5 a) and b) that for certain region of 4th generation particles and higgs masses the quality of the fit can be even better than in SM. According to the results of [11] the $\chi^2/n_{d.o.f.}(SM) = 1.09$, which corresponds to 2σ level, while in the presence of 4th generation it is $\chi^2_{min}/n_{d.o.f.} = 0.88$, which is inside 1σ region.

We should note, that the direct search of heavy neutrinos in e^+e^- annihilation into a pair of heavy neutrinos with the emission of the initial state bremsstrahlung photon ($e^+e^- \to \gamma + Nothing$) could result in the bound $m_N \geq 50$ GeV [3, 4] if all four LEP experiments will make a combined analysis [6].

Though this bound on m_N would be slightly better than the one, obtained in the present paper, the data and the procedure used to extract the bounds are completely different and independent.

6 Conclusions.

In the present paper we analyzed the dependence of Z-lineshape on the location of the threshold of $N\bar{N}$ production. We studied the behavior of $e^+e^- \to hadrons$ cross section near the threshold of $N\bar{N}$ production and determined how this threshold changes the Z-lineshape. In order to find the bound on m_N, we compared the theoretical predictions for the Z-lineshape with the experimental data, using the exact formulae for Z polarization operator, instead of expanding it into a Taylor series near m_Z.

We found that the bound on N mass depends on the higgs mass and the splittings of 4th generation quark and lepton masses ($|m_U - m_D|$ and $|m_E - m_N|$). However, the effects caused by them are not independent, because the increase of mass splittings can be compensated by the increase of the higgs mass, as it was shown in [5]. Using the results of [5] we fixed $m_E = 100$ GeV. Then we used the fact that $|m_U - m_D|$ and m_H are not independent. Thus, we had one free parameter left: $|m_U - m_D|$. We varied $|m_U - m_D|$ from 0 to 50 GeV and found that the 4th generation is excluded by the experimental data at 95% C. L. for $m_N < 46.7 \pm 0.2$ GeV. The theoretical uncertainty is caused by the varying of $|m_U - m_D|$, as well as by the uncertainties of the input parameters of ZFITTER, which were also used when calculating σ_h and σ_h^{SM}.

References

[1] N. Evans, Phys. Lett. **B340** (1994) 81;
P. Bamert and C. P. Burgess, Z. Phys. **C66** (1995) 495;
T. Inami *et al.*, Mod. Phys. Lett. **A10** (1995) 1471;
A. Masiero *et al.*, Phys. Lett. **B355** (1995) 329;
V. A. Novikov *et al.*, Mod. Phys. Lett. **A10** (1995) 1915;
J. Erler, P. Langacker, Review of Particle Physics. The European Physical Journal **C15** (2000) 95, chapter 10.6.

[2] M. Maltoni, V. A. Novikov, L. B. Okun, A. N. Rozanov, and M. I. Vysotsky, Phys. Lett. **B476** (2000) 107.

[3] V.A. Ilyin *et al.*, Phys. Lett., **B503** (2001) 126; hep-ph/0006324;
V.A. Ilyin *et al.*, Proceedings ICHEP2000 Osaka conference; hep-ph/0009167.

[4] V. A. Novikov *et al.*, Phys. Lett. **B529** (2002) 111; hep-ph/0111028.

[5] V. A. Novikov *et al.*, JETP Lett. **76** (2002) 119; hep-ph/0203132.

[6] The ALEPH Collaboration, ALEPH 2001-010; CONF 2001-007 (2001); P.Abreu *et al.*, DELPHI Collaboration, Eur. Phys. J. **C16** (2000) 53; M. Acciari *et al.*, L3 Collaboration, Phys. Lett. **B470** (1999) 268; G. Abbiendi *et al.*, OPAL Collaboration, Eur. Phys. J. **C14** (2000) 73.

[7] H.-J. He, N. Polonsky and S. Su, Phys. Rev. **D64** (2001) 053004; hep-ph/0102144.

[8] V. A. Novikov *et al.*, Rep. Prog. Phys. **62** (1999) 1275.

[9] L. D. Landau, E. M. Lifshitz, Quantum Mechanics (Moscow, Nauka, 1974) par. 147.

[10] A. I. Baz, L. B. Okun, JETP **8** (1959) 526.

[11] LEP collaborations, Combination procedure for the precise determination of Z boson parameters from results of the LEP experiments, CERN-EP/2000-153; hep-ex/0101027.

[12] D. Bardin *et al.*, Comput. Phys. Commun., **133** (2001) 229.

[13] ALEPH Coll., Phys. Lett., **B429** (1998) 201.

Table 1.

The experimental values of the $e^+e^- \to hadrons$ cross section, obtained by ALEPH, DELPHI, L3 and OPAL collaborations, extracted from Fig. 2 of [11]. $\sqrt{s}$ is presented in GeV, σ_h in nanobarns. The 1993-1995 data set.

Table 1.1 ALEPH

$\sqrt{s}$	89.4316	89.4400	91.1860	91.1980	91.2200	91.2840
σ_h	9.891	9.980	30.500	30.43	30.458	30.555
$\delta\sigma_h$	0.043	0.044	0.078	0.032	0.067	0.13

$\sqrt{s}$	91.2950	91.3030	92.9685	93.0140
σ_h	30.678	30.660	14.300	14.04
$\delta\sigma_h$	0.078	0.090	0.060	0.056

Table 1.2 DELPHI

$\sqrt{s}$	89.4307	89.4378	91.186	91.2	91.203	91.28
σ_h	9.87	9.93	30.392	30.50	30.46	30.65
$\delta\sigma_h$	0.044	0.056	0.065	0.044	0.19	0.13

$\sqrt{s}$	91.292	91.304	92.966	93.014
σ_h	30.67	30.46	14.35	13.89
$\delta\sigma_h$	0.098	0.086	0.044	0.045

Table 1.3 L3

$\sqrt{s}$	89.4497	89.4515	91.206	91.222	91.297	91.309
σ_h	10.088	10.08	30.358	30.547	30.525	30.545
$\delta\sigma_h$	0.034	0.034	0.067	0.034	0.087	0.067

$\sqrt{s}$	92.983	93.035
σ_h	14.231	13.91
$\delta\sigma_h$	0.046	0.053

Table 1.4 OPAL

$\sqrt{s}$	89.4415	89.45	91.207	91.222	91.285	92.973	93.035
σ_h	9.980	10.044	30.445	30.46	30.64	14.27	13.85
$\delta\sigma_h$	0.044	0.034	0.053	0.025	0.098	0.046	0.046